Cassini encounters with hot flow anomaly-like phenomena at Saturn's bow shock

A. Masters,[1] C. S. Arridge,[2,3] M. K. Dougherty,[1] C. Bertucci,[1] L. Billingham,[1] S. J. Schwartz,[1] C. M. Jackman,[1] Z. Bebesi,[4] A. J. Coates,[2,3] and M. F. Thomsen[5]

Received 16 October 2007; accepted 11 December 2007; published 18 January 2008.

[1] The first observations of the kronian equivalent of hot flow anomalies (HFAs) are presented. Using magnetic field and plasma data we discuss two events that were observed upstream of Saturn's bow shock during the first two orbits of the Cassini spacecraft. We suggest that these events result from the interaction between interplanetary current sheets and the shock surface. This same interaction is responsible for HFAs at the terrestrial bow shock. Calculations of electron temperature reveal an increase by a factor of approximately two for the first event, which is less than for terrestrial HFAs where the increase is by approximately an order of magnitude. In contrast to terrestrial HFAs we find that these events are associated with density enhancement rather than reduction. Estimates of the total pressure for the first event imply that the central region is expanding. **Citation:** Masters, A., C. S. Arridge, M. K. Dougherty, C. Bertucci, L. Billingham, S. J. Schwartz, C. M. Jackman, Z. Bebesi, A. J. Coates, and M. F. Thomsen (2008), Cassini encounters with hot flow anomaly-like phenomena at Saturn's bow shock, *Geophys. Res. Lett.*, *35*, L02202, doi:10.1029/2007GL032371.

1. Introduction

[2] The bow shock wave resulting from the interaction between the supermagnetosonic solar wind and a magnetized planet is associated with a number of magnetic field and plasma perturbations. Regions of hot, rarefied, strongly deflected solar wind plasma upstream of the Earth's bow shock were first observed in the mid-1980s by the AMPTE and ISEE spacecraft [*Schwartz et al.*, 1985; *Thomsen et al.*, 1986], these phenomena are now called hot flow anomalies (HFAs). An HFA is a perturbation of the bow shock caused by the interaction between the shock and an interplanetary current sheet. Present understanding of HFA formation [*Burgess and Schwartz*, 1988; *Thomsen et al.*, 1988] suggests that the solar wind motional electric field focuses ions that have been reflected at the shock onto the current sheet. Ion-ion instabilities [*Gary*, 1991] result in a region of heated solar wind plasma that then expands.

[3] Observationally HFAs are characterized by this expanding region with flanking compression regions and an underlying interplanetary magnetic field (IMF) discontinuity [*Lepping and Behannon*, 1986]. The heated plasma shows a strong deflection from the nominal direction of solar wind flow and the electron and ion distributions are approximately Maxwellian [*Lucek et al.*, 2004]. Due to the expansion of the cavity there is also a density decrease in the central region, with the plasma pressure sustained by the temperature increase.

[4] *Schwartz et al.* [2000] discussed the conditions for the formation of HFAs at the Earth's bow shock and estimated that several HFAs should occur per day. It has been shown that HFAs can convect into the magnetosheath [*Šafránková et al.*, 2000] and *Sibeck et al.* [1999] documented an HFA that caused a displacement of the Earth's magnetopause by approximately 5 Earth radii and an auroral brightening. The implication of these studies is that HFAs occur frequently, can affect the magnetopause and can cause a ground response. Thus HFAs may play an important role in terrestrial magnetospheric dynamics.

[5] The properties of the bow shock and solar wind at Saturn are significantly different to those at Earth. The fast magnetosonic Mach number of Saturn's bow shock is typically 13 [*Achilleos et al.*, 2006], which is high compared to that of the Earth's bow shock which is typically 7 [*Peredo et al.*, 1995]. From Earth to Saturn orbit the magnitude of the IMF and solar wind density drop by approximately two orders of magnitude [*Jackman et al.*, 2005] and the Parker spiral angle increases from $\sim 45°$ to $\sim 85°$. Despite these differences it is possible in principle that the interaction between interplanetary current sheets and Saturn's bow shock could also generate HFAs. Importantly, *Øieroset et al.* [2001] demonstrated that HFAs are not an exclusively terrestrial phenomenon by identifying them at the Martian bow shock.

[6] The determination of whether or not HFAs occur at Saturn's bow shock could be important for our understanding of Saturn's magnetospheric dynamics. The Cassini spacecraft has made observations upstream of the shock, allowing us to carry out a thorough investigation. In this paper we outline how we searched for the kronian analogue of HFAs and we discuss the observations of the two events that were identified.

2. Observations

[7] To identify the kronian equivalent of HFAs we inspected one second resolution magnetic field data taken

[1]Space and Atmospheric Physics Group, Blackett Laboratory, Imperial College London, London, U. K.
[2]Mullard Space Science Laboratory, Department of Space and Climate Physics, University College London, Dorking, U. K.
[3]Centre for Planetary Sciences, University College London, London, U. K.
[4]KFKI Research Institute for Particle and Nuclear Physics, Budapest, Hungary.
[5]Space Science and Applications, Los Alamos National Laboratory, Los Alamos, New Mexico, USA.

Copyright 2008 by the American Geophysical Union.
0094-8276/08/2007GL032371

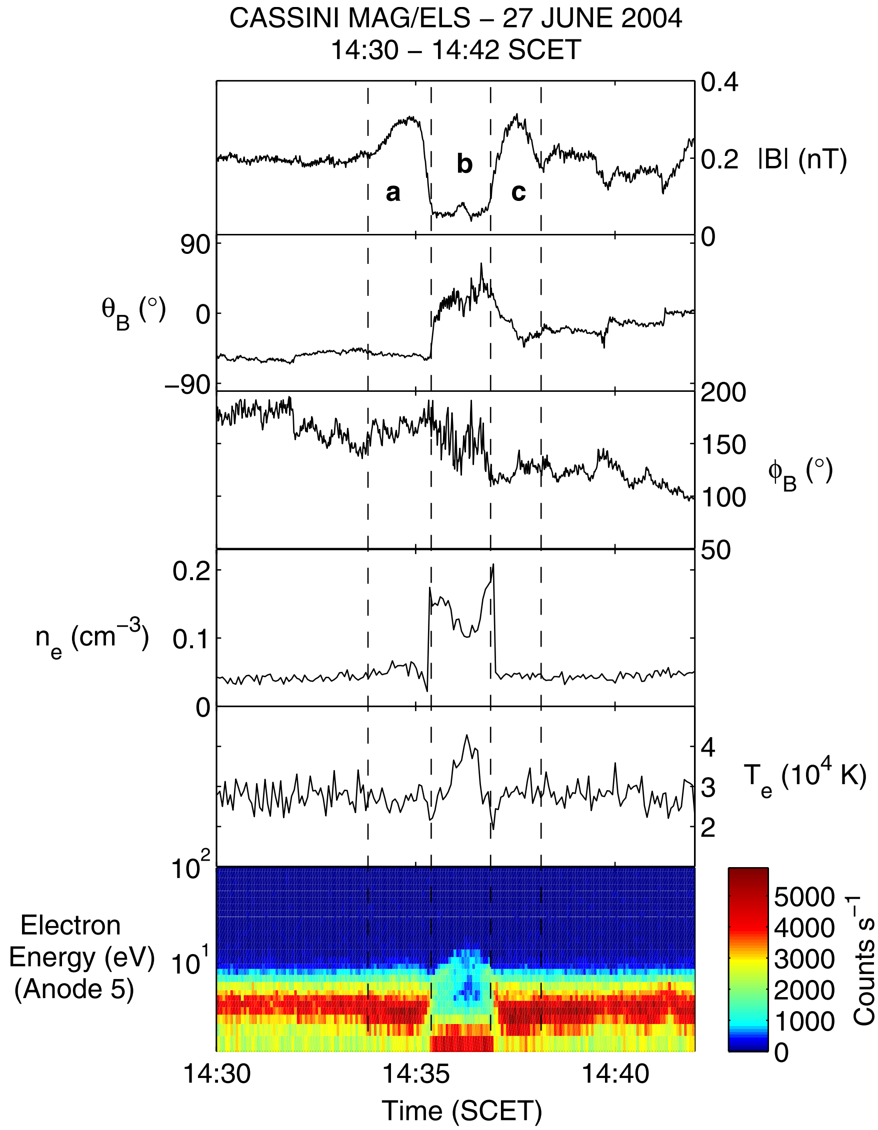

Figure 1. MAG and ELS data for a 12 minute interval surrounding the first event.

by the fluxgate magnetometer of the Cassini dual technique magnetometer [*Dougherty at al.*, 2004]. We inspected the data taken upstream of the bow shock during the first two Saturn orbits and identified relatively rapid changes in the direction of the magnetic field vector that are indicative of spacecraft encounters with IMF discontinuities. We then chose the events where the encounter with the discontinuity was associated with a disturbance to the nominal magnitude of the IMF. This left us with the two events that we present in this paper. We analysed the magnetic field and corresponding plasma data, taken by the electron spectrometer sensor (ELS) and ion beam spectrometer (IBS) of the Cassini plasma spectrometer [*Young et al.*, 2004], to determine the particle dynamics during each event.

2.1. Event 1: 27 June 2004

[8] The first event occurred on 27 June 2004 during the inbound pass of the first orbit at around 14:36 spacecraft event time (SCET). The event took place at a range of 47.0 R_S (1 R_S = 60268 km), and was in the post-dawn sector at a Saturn Local Time (SLT) of 07:50. Since the bow shock moves much faster than the spacecraft as it responds to changes in the solar wind dynamic pressure [*Achilleos et al.*, 2006], multiple crossings of the shock can be observed in a pass. During this particular pass Cassini crossed the shock seven times and the event occurred when the spacecraft was in the solar wind between the second and third crossings, suggesting that the event took place in close proximity to the shock.

[9] Figure 1 shows the magnetic field and plasma data for a 12 minute interval surrounding the event. The top three panels show the magnitude and direction of the magnetic field in spherical polar coordinates. The fourth and fifth panels are the electron number density and temperature respectively (deduced from CAPS ELS) and the sixth (bottom) panel is a time-energy spectrogram of electron counts from ELS anode 5. The dashed lines separate the intervals labelled *a*, *b* and *c* in the top panel. In the typical field magnitude signature of terrestrial HFAs an enhancement-depression-enhancement pattern is observed. The field

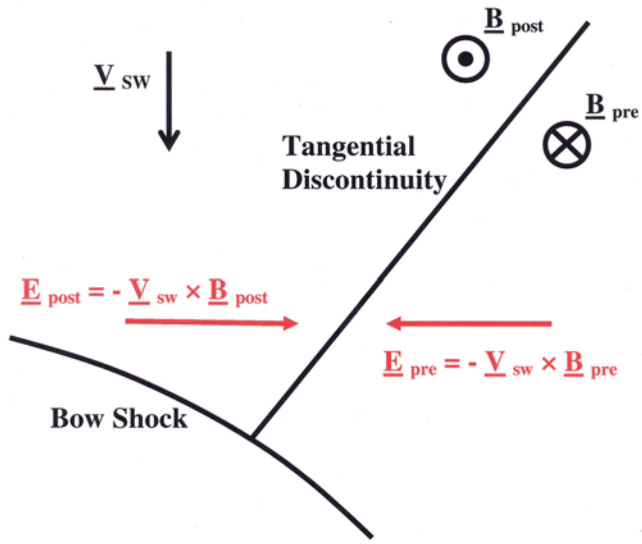

Figure 2. Schematic illustrating the interaction between an interplanetary tangential discontinuity and the bow shock required for HFA formation (adapted from *Schwartz et al.* [2000]).

enhancements and depression correspond to compression regions and a cavity of heated solar wind plasma respectively. This profile is present in the field magnitude signature of this first event and so the intervals in Figure 1 have been identified to examine if they correspond to the same plasma features as for terrestrial HFAs.

[10] The field angles change during the event, resulting in a magnetic field vector rotation of $\sim$61.2°, which suggests that an IMF discontinuity underlies the event. The electron number density and temperature are relatively constant apart from during interval *b* where there is an increase in electron temperature from $\sim(2.5 \times 10^4)$ K to $\sim(4.0 \times 10^4)$ K and an increase in electron number density from $\sim$0.05 cm^{-3} to $\sim$0.15 cm^{-3}. In contrast to terrestrial HFAs, regions *a* and *c* (the regions of field magnitude enhancement) do not correspond to density increases. This distinctive electron population in region *b* is clear in the time-energy spectrogram. Spacecraft photoelectrons and ambient electrons are observed below an energy of $\sim$10 eV throughout the interval. However in region *b* there is an increase in the count rate above 10eV and the peak of the photoelectron distribution shifts from $\sim$5 eV to $\sim$2 eV. The increased count rate above 10 eV is due to the increased temperature of the ambient electron population. The shift in the peak of the photoelectron distribution is caused by an increase in the return current to the spacecraft as it becomes immersed in a hotter, denser ambient electron population [*Ishisaka et al.*, 2001]. During the event the solar wind ion flow did not lie in the field of view of the IBS instrument and so ion moments are not available.

[11] The development of this heated population disturbs the IMF leading to the breakdown of the original IMF discontinuity. The initial discontinuity is implied by the change in the orientation of the field over the event, but a determination of the nature of the underlying discontinuity is not possible. For terrestrial HFAs there is observational and simulational evidence that the underlying discontinuity is a tangential discontinuity (TD) [*Sibeck et al.*, 1999; *Thomas et al.*, 1991]. Thus studies at Earth have assumed this and have calculated the normal to the TD plane as the vector product of the magnetic field either side of the disturbance [*Schwartz et al.*, 2000].

[12] In this study we make the same assumption and use the average field in a three minute interval before and after the event. The resulting TD plane normal makes an angle of $\sim$35.7° to the Saturn-Sun line. Minimum variance analysis (MVA) [*Sonnerup and Schreible*, 1998] applied to the boundaries of the event to calculate their orientation was considered, however the results were inconclusive due to eigenvalue ratios below 10. To investigate the physics of the interaction region between the underlying discontinuity and the shock we carried out further analysis of the magnetic field data. Once again we used the same approach that has been used to study terrestrial HFAs; Figure 2 illustrates the method. The schematic shows the intersection between the TD and the bow shock, the direction of the solar wind flow, and the magnetic field and solar wind motional electric field ($E = -V_{SW} \times B$) either side of the intersection.

[13] For a terrestrial HFA to form the solar wind motional electric field on at least one side has to have a component directed towards the underlying discontinuity [*Thomsen et al.*, 1993]. Under these circumstances a population of shock-reflected, gyrating ions will be guided into the upstream region along the discontinuity and lead to the formation of an HFA [*Burgess and Schwartz*, 1988; *Thomsen et al.*, 1988]. A gyrating ion population is associated with a quasi-perpendicular shock; this is where the angle between the shock normal and the upstream magnetic field (θ_{Bn}) is >45° [*Gosling and Robson*, 1985].

[14] To examine whether this requirement is satisfied for this event we calculated the solar wind motional electric field ($E = -V_{SW} \times B$) either side of the event and scaled a model for Saturn's bow shock to the approximate event position. Due to pointing constraints it was not possible to obtain reliable measurements of the solar wind speed and so we assumed $V_{SW} = (500 \pm 100)$ km s^{-1} in the anti-sunward direction, since this is typical of the solar wind at Saturn [*Crary et al.*, 2005]. The model bow shock used was the hyperbolic surface constructed by *Slavin et al.* [1985]. We find that the angle between the motional electric field and the TD normal on the pre-event side is $\sim$75.7° and on the post-event side it is $\sim$24.7°. The motional electric field has a component directed towards the underlying discontinuity on both sides. Using the Slavin model local shock normal, we calculate $\theta_{Bn} \sim 56.3°$ on the pre-event side and $\theta_{Bn} \sim 40.6°$ on the post-event side. Although neither θ_{Bn} is significantly higher than 45° there will still be a population of gyrating ions in front of the shock, particularly on the side where $\theta_{Bn} \sim 56.3°$ [*Gosling and Robson*, 1985].

[15] These results suggest that at the intersection between the underlying discontinuity and the shock a population of shock-reflected gyrating ions is present on at least one side of the intersection, and on both sides the motional electric field focuses these ions onto the discontinuity. A further condition for the formation of HFAs at the Earth's bow shock concerns the speed at which the discontinuity tracks across the shock surface. *Schwartz et al.* [2000] derived an expression for the ratio between that speed and the speed of

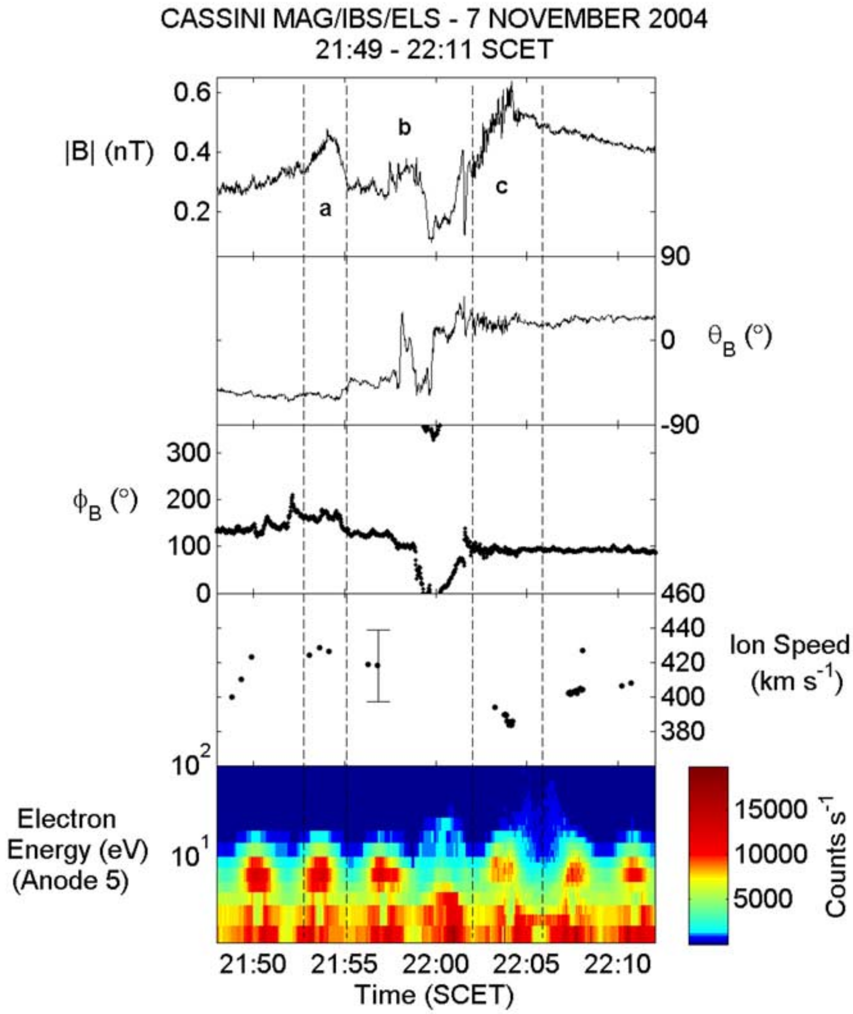

Figure 3. MAG, IBS and ELS data for a 22 minute interval surrounding the second event.

an ion gyrating in front of the shock. This provides a measure of whether the gyrating ions have time to reach the discontinuity. A value less than one, as found at terrestrial HFAs, implies that the discontinuity tracks across the surface sufficiently slowly for an HFA to be generated. For this event we calculate the ratio to be $\sim$0.68. We conclude that the characteristics of the IMF discontinuity and its interaction with the bow shock satisfy the conditions for the formation of terrestrial HFAs [*Schwartz et al.*, 2000].

[16] To complete our analysis we considered the dynamics of this region of heated plasma and estimated the size of the event. Assuming an ion number density and temperature equal to that of the electrons we calculated the sum of the magnetic and plasma pressures to be $\sim(1.7 \times 10^{-4})$ nPa inside region *b* of Figure 1, and $\sim(7.0 \times 10^{-5})$ nPa in regions *a* and *c*. The sum of the pressures inside region *b* is $\sim$2.4 times greater than in regions *a* and *c*, implying that the central region was expanding due to the pressure gradient force at the time of the encounter. For terrestrial HFAs the ions are typically an order of magnitude hotter than the electrons in the central region. If the same process that generates terrestrial HFAs is responsible for this event we would expect the sum of the pressures to be greater than the value calculated in interval *b*. We determine the plasma β (ratio of plasma to magnetic pressure) to be $\sim$128.1 in region *b* and $\sim$1.0 in regions *a* and *c*; this is in agreement with observations of terrestrial HFAs [*Thomsen et al.*, 1986]. As the event is convected over the spacecraft by the solar wind, assuming a solar wind speed of 500 km s^{-1}, the approximate spatial extent of the event (beginning of region *a* to end of region *c*) along the solar wind flow direction is $\sim$2.1 R_S.

2.2. Event 2: 7 November 2004

[17] We now present a second event that occurred on 7 November 2004 after the last shock crossing of the outbound pass of the second orbit at around 22:00 SCET. The event took place at a range of 60.6 R_S and was in the pre-dawn sector at an SLT of 05:48. Since the event occurs at a range and SLT where we typically observe the shock it is possible that the event occurred in close proximity to the shock.

[18] Figure 3 shows the magnetic field and plasma data for a 22 minute interval surrounding the event. The top three panels are the magnitude and direction of the magnetic field in spherical polar coordinates, the fourth panel is the IBS

ion speed and the fifth (bottom) panel is a time-energy spectrogram of electron counts from ELS anode 5. In the fourth panel an error bar is plotted on one point that is typical of all the points (±20 km s^{-1}). The dashed lines separate the intervals labelled *a*, *b* and *c* that were identified using the same criteria as for the first event. During this interval the ELS sensor was actuating and this led to the observed periodic modulation of the time-energy spectrogram. The actuation prohibits a straight-forward calculation of the moments of the ambient electron distribution, however the solar wind ion flow was in the field of view of the IBS sensor at the time and so ion data is available. Although low IBS count rates are observed, whenever there are a sufficient number of counts the ion speed is calculated by assuming a Gaussian distribution. The error is given by the difference between the velocity corresponding to the peak of the Gaussian fit and the velocity corresponding to the energy channel with the highest count rate.

[19] This second event has similar observational characteristics to the first. The field angles change during the event; the magnetic field rotates by ~88.5°. This suggests the presence of an underlying IMF discontinuity. There is a cluster of measurements of ion speed associated with region *c* that are below the average for the interval. We suggest this is due to the motion of the plasma along the discontinuity with a component against the solar wind flow, resulting in a decrease in ion speed that is characteristic of terrestrial HFAs [*Thomsen et al.*, 1986]. However we note that firm conclusions regarding the flow deflection cannot be drawn due to the scarcity of points, magnitude of the errors and lack of measurements in region *b* where the speed reduction is expected to be clearest.

[20] Spacecraft photoelectrons and ambient electrons are observed below ~11 eV in the spectrogram. Despite the actuation it is clear that in region *b* the peak of the photoelectron distribution shifts to a lower energy and there is an increase in the count rate above 11 eV. These features are similar to the features of the spectrogram for the first event and we suggest that they are caused by the presence of an ambient plasma in region *b* with similar properties. The shift in the photoelectron distribution peak indicates a decrease in the spacecraft potential, implying that the temperature and density of the ambient electrons in region *b* is greater than in the surrounding solar wind plasma [*Ishisaka et al.*, 2001]. Another increase in the count rate above 11 eV coincides with region *c*. We suggest that on this side the expansion of region *b* drives a weak shock and these higher energy electrons may be associated with shock heating [*Schwartz et al.*, 1988].

[21] We assumed that the underlying discontinuity is a TD and calculated the TD normal by taking the vector product of the average magnetic field in three minute intervals either side of the disturbance. As for the first event, the MVA results were inconclusive. The analysis that was applied to the first event was also carried out on this second event and the results imply that the solar wind motional electric field only has a component directed towards the underlying discontinuity on the post-event side (angle between motional electric field and TD normal: ~64.4°). On this same side θ_{Bn} ~67.1° which suggests a quasi-perpendicular shock geometry. The ratio of intersection tracking speed to that of a gyrating ion is ~0.75, suggesting a sufficiently slow tracking speed. Therefore this event also satisfies terrestrial HFA formation conditions. Finally, by assuming an anti-sunward solar wind flow at 500 km s^{-1} we estimate the spatial extent of the event (beginning of region *a* to end of region *c*) along the solar wind flow direction to be ~6.4 R_S.

3. Conclusions

[22] Observations of two events that occurred upstream of Saturn's bow shock have been presented. We have demonstrated that each results from the interaction between an interplanetary current sheet and the shock. The conditions for the formation of HFAs at the terrestrial bow shock are satisfied for both events and we suggest that the central region of the first event is expanding. The plasma data corresponding to the first event reveals an increase in electron temperature that is less dramatic than that measured at terrestrial HFAs. A difference between these events and their terrestrial counterparts is that an increase in density takes place in the central region, whereas at terrestrial HFAs a decrease occurs. We propose that these events are examples of the kronian equivalent of HFAs.

[23] Future work will involve the identification of further events associated with extensive ion data. An understanding of the behaviour of the ions is necessary to provide further evidence that these events form by the same process that results in HFAs at Earth. As these events become better understood a discussion of the role they play in magnetospheric dynamics will be made possible.

[24] **Acknowledgments.** AM acknowledges useful discussions with E. A. Lucek, T. S. Horbury, N. Achilleos, and E. M. Henley, as well as the support of the Royal Astronomical Society. We acknowledge the support of the MAG data processing/distribution staff and L. K. Gilbert and G. R. Lewis for ELS data processing. This work was supported by UK STFC through the award of studentships (AM, LB), a Post-Doctoral Fellowship (CB) and research grants to MSSL/UCL and Imperial College London.

References

Achilleos, N., et al. (2006), Orientation, location and velocity of Saturn's bow shock: Initial results from the Cassini spacecraft, *J. Geophys. Res.*, *111*, A03201, doi:10.1029/2005JA011297.

Burgess, D., and S. J. Schwartz (1988), Colliding plasma structures: Current sheet and perpendicular shock, *J. Geophys. Res.*, *93*, 11,327.

Crary, F. J., et al. (2005), Solar wind dynamic pressure and electric field as the main factors controlling Saturn's aurorae, *Nature*, *433*, 720.

Dougherty, M. K., et al. (2004), The Cassini magnetic field investigation, *Space Sci. Rev.*, *114*, 331.

Gary, S. P. (1991), Electromagnetic ion/ion instabilities and their consequences in space plasmas: A review, *Space Sci. Rev.*, *56*, 373.

Gosling, J. T., and A. E. Robson (1985), Ion reflection, gyration, and dissipation at supercritical shocks, in *Collisionless Shocks in the Heliosphere: Reviews of Current Research*, *Geophys. Monogr. Ser.*, vol. 35, edited by B. T. Tsurutani and R. G. Stone, p. 141, AGU, Washington, D. C.

Ishisaka, K., T. Okada, K. Tsuruda, H. Hayakawa, T. Mukai, and H. Matsumoto (2001), Relationship between the Geotail spacecraft potential and the magnetospheric electron number density including the distant tail regions, *J. Geophys. Res.*, *106*, 6309.

Jackman, C. M., et al. (2005), Structure of the interplanetary magnetic field during the interval spanning the first Cassini fly-through of Saturn's magnetosphere and its implications for Saturn's magnetospheric dynamics, *Adv. Space. Res.*, *36*, 2120.

Lepping, R. P., and K. W. Behannon (1986), Magnetic field directional discontinuities: Characteristics between 0.46 and 1.0 AU, *J. Geophys. Res.*, *91*, 8725.

Lucek, E. A., T. S. Horbury, A. Balogh, I. Dandouras, and H. Rème (2004), Cluster observations of hot flow anomalies, *J. Geophys. Res.*, *109*, A06207, doi:10.1029/2003JA010016.

Øieroset, M., D. L. Mitchell, T. D. Phan, R. P. Lin, and M. H. Acuña (2001), Hot diamagnetic cavities upstream of the Martian bow shock, *Geophys. Res. Lett.*, *28*(5), 887.
Peredo, M., J. A. Slavin, E. Mazur, and S. A. Curtis (1995), Three-dimensional position and shape of the bow shock and their variation with Alfvénic, sonic, and magnetosonic Mach numbers and interplanetary magnetic field orientation, *J. Geophys. Res.*, *100*, 7907.
Šafránková, J., L. Přech, Z. Němeček, D. G. Sibeck, and T. Mukai (2000), Magnetosheath response to the interplanetary magnetic field tangential discontinuity, *J. Geophys. Res.*, *105*, 25,113.
Schwartz, S. J., et al. (1985), An active current sheet in the solar wind, *Nature*, *318*, 269.
Schwartz, S. J., M. F. Thomsen, S. J. Bame, and J. Stansberry (1988), Electron heating and the potential jump across fast mode shocks, *J. Geophys. Res.*, *93*, 12,923.
Schwartz, S. J., G. Paschmann, N. Sckopke, T. M. Bauer, M. Dunlop, A. N. Fazakerley, and M. F. Thomsen (2000), Conditions for the formation of hot flow anomalies at Earth's bow shock, *J. Geophys. Res.*, *105*, 12,639.
Sibeck, D. G., et al. (1999), Comprehensive study of the magnetospheric response to a hot flow anomaly, *J. Geophys. Res.*, *104*, 4577.
Slavin, J. A., E. J. Smith, J. R. Spreiter, and S. S. Stahara (1985), Solar wind flow about the outer planets: Gas dynamic modeling of the Jupiter and Saturn bow shocks, *J. Geophys. Res.*, *90*, 6275.
Sonnerup, B. U. O., and M. Schreible (1998), Minimum and maximum variance analysis, in *Analysis Methods for Multi-Spacecraft Data*, edited by G. Paschmann and P. W. Daly, ISSI Sci. Rep. SR-001, ESA Publ. Div., Noordwijk, Netherlands.
Thomas, V. A., D. Winske, M. F. Thomsen, and T. G. Onsager (1991), Hybrid simulation of the formation of a hot flow anomaly, *J. Geophys. Res.*, *96*, 11,625.
Thomsen, M. F., J. T. Gosling, S. A. Fuselier, S. J. Bame, and C. T. Russell (1986), Hot, diamagnetic cavities upstream from the Earth's bow shock, *J. Geophys. Res.*, *91*, 2961.
Thomsen, M. F., J. T. Gosling, S. J. Bame, K. B. Quest, C. T. Russell, and S. A. Fuselier (1988), On the origin of hot diamagnetic cavities near the Earth's bow shock, *J. Geophys. Res.*, *93*, 11,311.
Thomsen, M. F., V. A. Thomas, D. Winske, J. T. Gosling, M. H. Farris, and C. T. Russell (1993), Observational test of hot flow anomaly formation by the interaction of a magnetic discontinuity with the bow shock, *J. Geophys. Res.*, *98*, 15,319.
Young, D. T., et al. (2004), Cassini plasma spectrometer investigation, *Space Sci. Rev.*, *114*, 1.

C. S. Arridge and A. J. Coates, Mullard Space Science Laboratory, Department of Space and Climate Physics, University College London, Holmbury St. Mary, Dorking, RH5 6NT, UK.

Z. Bebesi, KFKI Research Institute for Particle and Nuclear Physics, 29–33 Konkoly Thege, H-1515, Budapest, Hungary.

C. Bertucci, L. Billingham, M. K. Dougherty, A. Masters, C. M. Jackman, and S. J. Schwartz, Space and Atmospheric Physics Group, Blackett Laboratory, Imperial College London, Prince Consort Road, London, SW7 2AZ, UK. (adam.masters02@imperial.ac.uk)

M. F. Thomsen, Space Science and Applications, Los Alamos National Laboratory, Los Alamos, NM 87545, USA.